

ReCo: Region-Controlled Text-to-Image Generation (Supplementary Material)

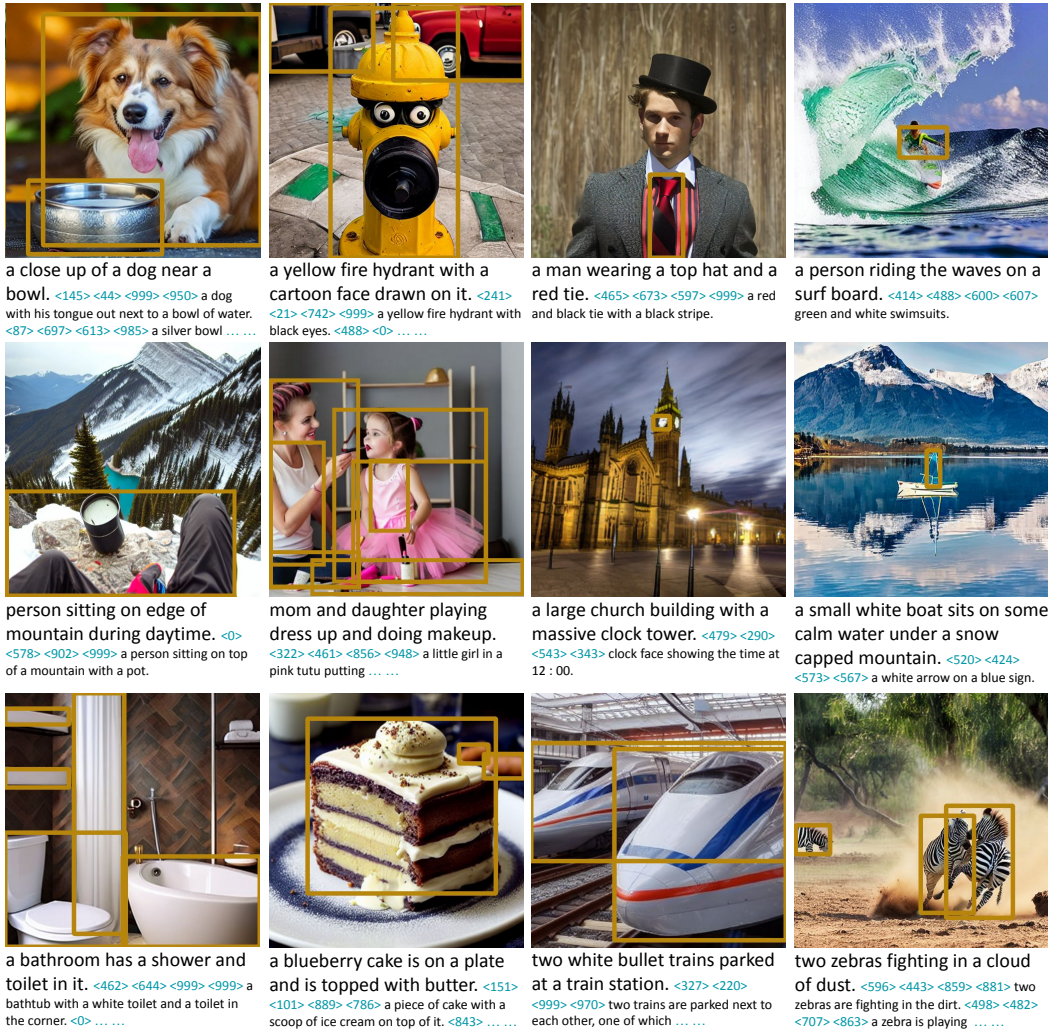


Figure A. Example images generated by ReCo_{LAION}. More examples are in Figures G, H.

A. ReCo with LAION data

In the main paper, we focus on the ReCo model trained on COCO (ReCo_{COCO}) to standardize the evaluation process. In this section, we present ReCo_{LAION} that conducts the same ReCo fine-tuning on a small subset of the LAION dataset [5] used by the pre-trained SD model [4]. Figure A shows selected ReCo_{LAION}-generated image samples.

Training setup. Instead of using the 414K image-text pairs (83K images) from the COCO 2014 training set, we randomly sample 100K images from the LAION-Aesthetics dataset¹. We take the Detic object detector [9] to generate

¹We use the first 100K samples with an aesthetics score of 6 or higher following the index in https://huggingface.co/datasets/ChristophSchuhmann/improved_aesthetics_6plus.

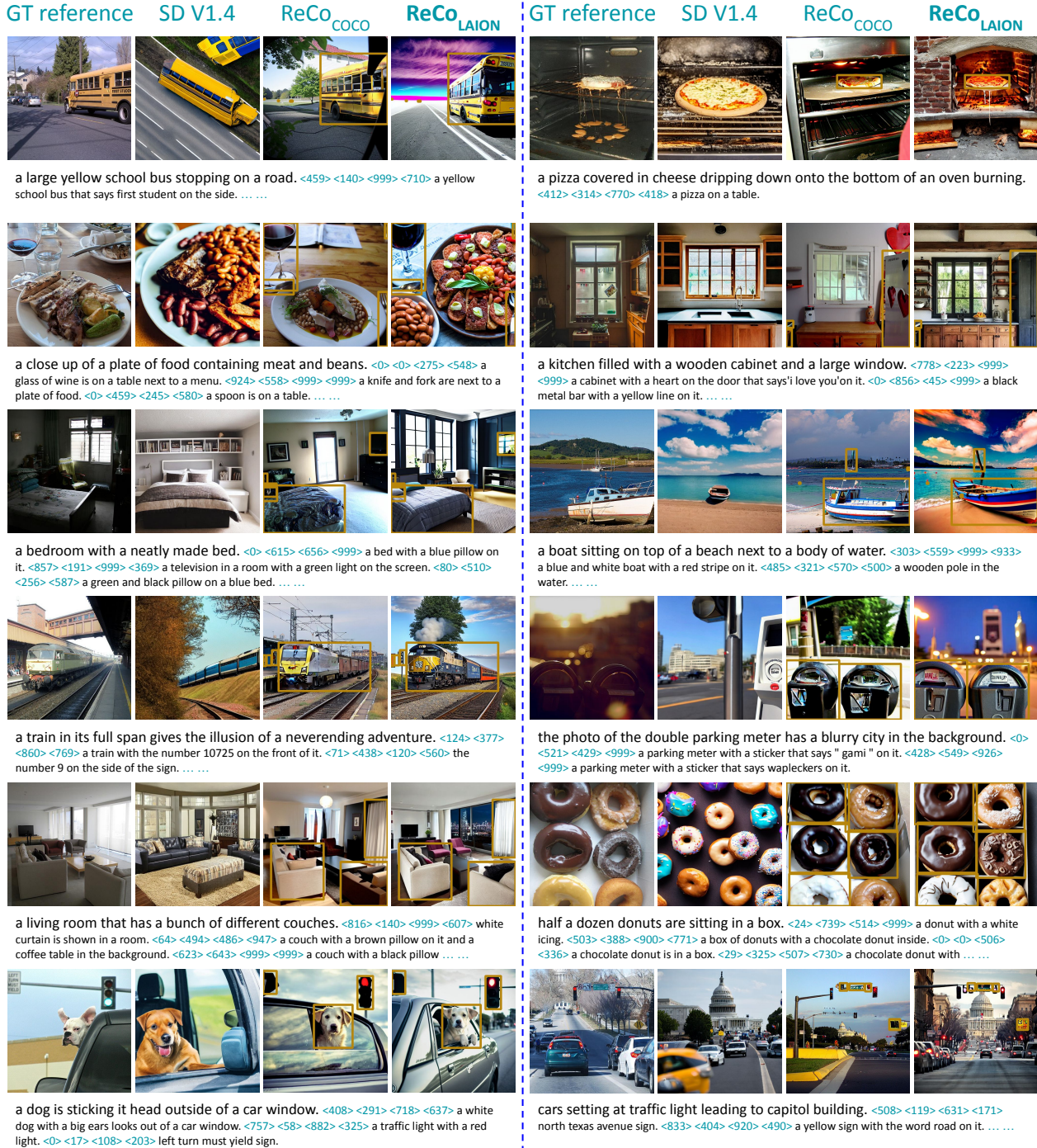


Figure B. Qualitative results on LVIS [2]. Zoomed-in version is in Figure G.

the object region predictions. We use a confidence threshold of 0.5 and filter out small boxes with a size smaller than $0.03 \times W \times H$. Following the setting for ReCo_{COCO}, we feed all cropped regions to the pre-trained GIT captioning model [6] for regional descriptions. We fine-tune ReCo for 10,000 steps with the same training and inference settings introduced in the main paper.

Qualitative results. Figure B shows qualitative results on

LVIS [2]. Both ReCo_{COCO} and ReCo_{LAION} show strong region-controlled T2I generation capabilities. Compared with ReCo_{COCO}, ReCo_{LAION}-generated images have better image aesthetic scores, thanks to the high-aesthetic fine-tuning data from LAION [5].

Figure C shows qualitative results on LAION-Aesthetics. We run T2I inference on 3K samples indexed after the first 100K samples used for ReCo fine-tuning.

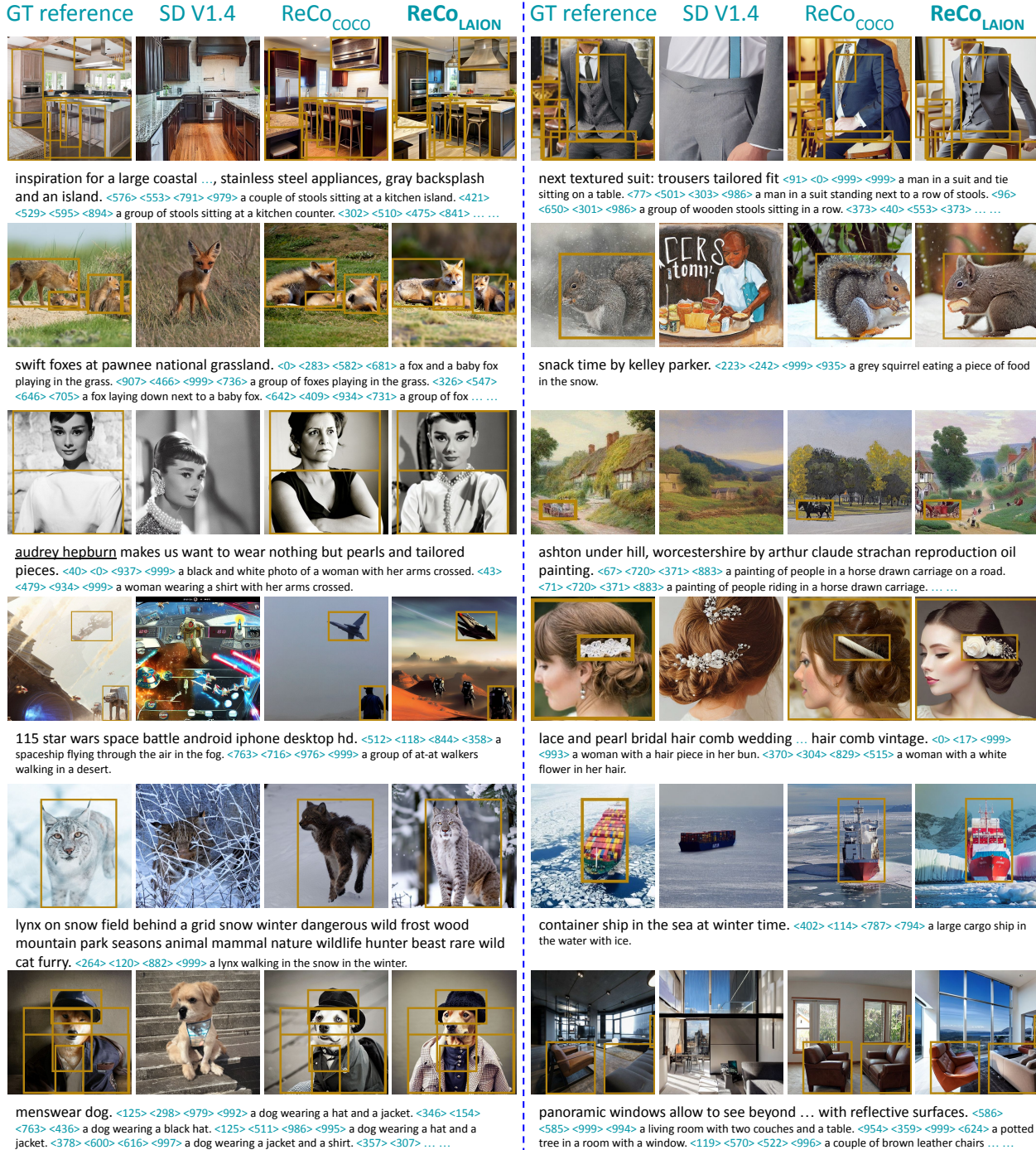
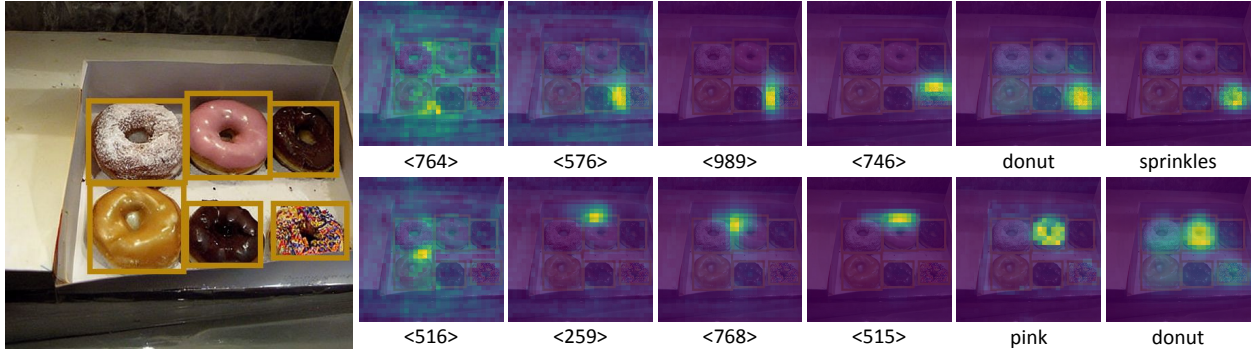


Figure C. Qualitative results on prompts selected from LAION-Aesthetics [5]. Zoomed-in version is in Figure H.

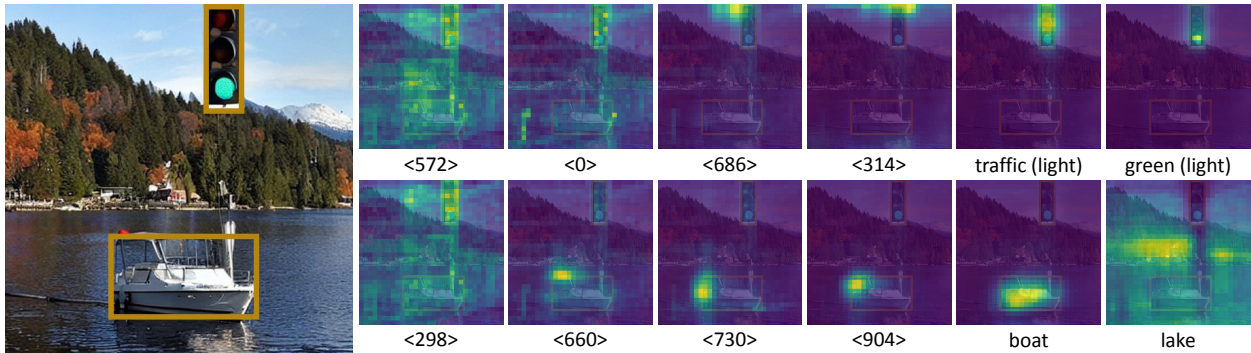
ReCo_{LAION} can preserve the pre-trained SD’s capabilities of understanding celebrities, art styles, and open-vocabulary descriptions, and meanwhile extend SD with the appealing new ability of region-controlled T2I generation.

Quantitative results. Table A compares ReCo_{LAION} with ReCo_{COCO} on LVIS [2]. The “COCO Image” column indicates if the COCO image style is seen during ReCo fine-tuning. Automatic metrics show that ReCo_{COCO} achieves

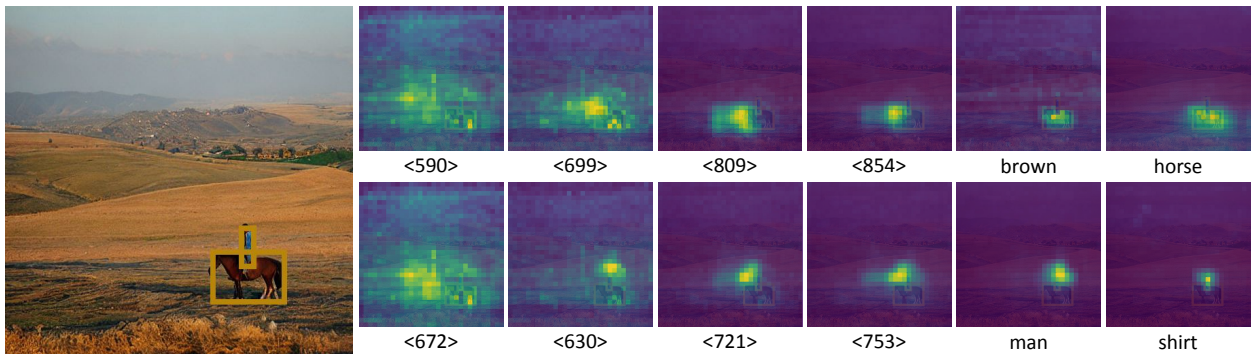
better region control accuracy and image FID. For region control, COCO ground-truth boxes provide a cleaner region specification than Detic-predicted boxes, thus benefiting the controlling accuracy. For the FID evaluation, ReCo_{COCO} has seen COCO images during ReCo training, leading to better FID scores. Qualitatively, ReCo_{LAION}-generated images show comparable, if not better visual qualities than ReCo_{COCO}. Overall, both ReCo model variants significantly



A box contains six donuts with varying types of glazes and toppings. <515> <576> <742> <766> chocolate donut. <237> <518> <521> <785> dark vanilla donut. <764> <576> <989> <746> donut with sprinkles. <234> <281> <525> <528> donut with powdered sugar. <516> <259> <768> <515> pink donut. <754> <289> <959> <507> brown donut.



A boat below a traffic light with a park in the background. <572> <0> <686> <314> a traffic light with the green light on. <298> <660> <730> <904> a white boat on the lake.



A zoomed out view of a man riding a horse through rural country side. <590> <699> <809> <854> brown horse. <672> <630> <721> <753> a man in blue shirt.

Figure D. Averaged ReCoCOCO cross-attention maps between visual latent and text embedding (on both text and position tokens).

Method	COCO Image	Object Acc. (↑)	SceneFID (↓)	FID (↓)
Real Images	-	42.00	-	-
SD V1.4	×	7.88	40.62	23.74
ReCoCOCO	✓	23.42	10.08	17.73
ReCoLAION	×	19.38	19.48	21.99

Table A. Evaluations on the images generated with the 4,809 LVIS validation samples [2] from COCO val2017. The object classification is conducted over the 1,203 LVIS classes.

outperform the original SD model in both region control accuracy and image generation quality.

B. Position Token Cross-Attention

To help interpret how the introduced position tokens operate, Figure D visualizes the cross-attention maps between the visual latent z and token embedding $\tau_\theta(y(P, T))$. We show the averaged attention maps across all diffusion steps and U-Net blocks. Similar to the cross-attention patterns observed in Pix2seq [1], we empirically observe that the four position tokens for each region help the model to progressively localize the specified area by attending to the corner or edge positions of the box region. These position tokens help text tokens to localize and focus on the detailed

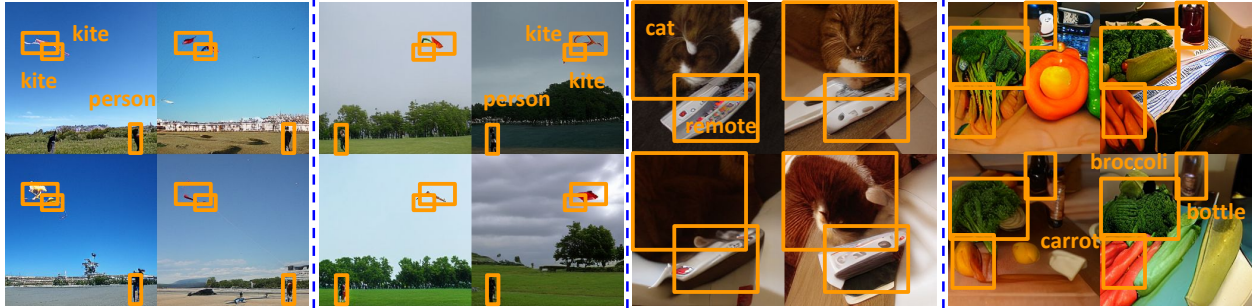
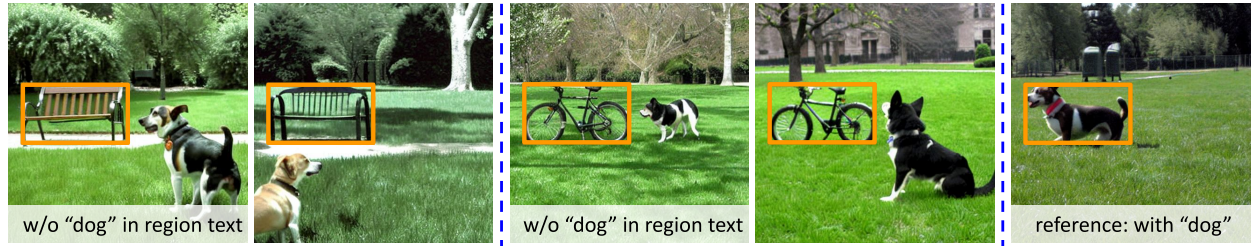


Figure E. ReCo_{OFA} based on the auto-regressive T2I model OFA_{Large} [7].



Region description: a chair in a park |

a bike in a park |

a dog in a park

Image description: A dog that is standing in the green grass. <54> <333> <505> <589> ...

Figure F. A case study of “inconsistent” image and region-level descriptions.

regional descriptions, *e.g.*, the “green light” in the “traffic light.” We hypothesize that the observed “coarse-to-fine-grained localization” pattern might be related to the causal masking in the text encoder, as early position tokens do not have the complete region information.

C. Supplementary Discussions

Generality beyond diffusion. In the main paper, we present ReCo based on the diffusion-based Stable Diffusion model [4]. To better understand if the core idea could generalize to other T2I systems, we conduct experiments with ReCo_{OFA}, a variation that uses an open-sourced auto-regressive T2I model OFA_{Large} [7] as the generation backbone. We empirically observe that ReCo’s capabilities and findings generalize well to auto-regressive T2I models (*cf.*, AP/AP₅₀/FID: ReCo_{OFA} 13.1/24.2/9.10 vs. OFA_{Large} 0.8/2.5/11.82). Specifically, ReCo’s region-controlled generation not only provides the desired region controllability but also improves the image generation quality. Figure E shows the results of ReCo_{OFA}’s region-controlled T2I generation.

“Inconsistent” image and region-level descriptions. Supporting both image and region-level descriptions may raise a natural question: What if the image-level description is inconsistent with the region-level descriptions? For example, the image description might mention a *dog*, but none of the region descriptions refer to the *dog*. Since texts typically provide only partial descriptions of images or image

Method	AP	AP ₅₀	Object Acc.	SceneFID	FID
ReCo	32.0	52.4	62.42	6.51	7.36
ReCo _{Position Word}	2.3	7.5	42.02	15.54	8.82
ReCo _{Relation Word}	1.5	4.8	43.99	13.98	9.50

Table B. Extending Table 1 with additional ReCo model variants.

patches, conflicts between image and region text descriptions may be rare in practice. As shown in Figure F, the model accommodates both image and region-level descriptions by properly drawing the *dog* outside of the box. We note that the model might still get confused with carefully engineered challenges, such as an image text stating “two dogs” paired with three “dog” regions. We leave those edge cases for future studies.

ReCo_{Relation Word} with relationship words. In addition to the position text words used in ReCo_{Position Word}, ReCo_{Relation Word} further includes the eleven object spatial relationships and their textual descriptions defined in previous studies [3, 8]. Table B shows mixed results when compared with ReCo_{Position Word}, while the performance remains lower than ReCo with position tokens. Therefore, we use ReCo_{Position Word} as the reference model in the main paper and propose that position tokens could be inherently more concise and accurate for spatial controllability.

References

- [1] Ting Chen, Saurabh Saxena, Lala Li, David J Fleet, and Geoffrey Hinton. Pix2seq: A language modeling framework for object detection. In *ICLR*, 2022. 4

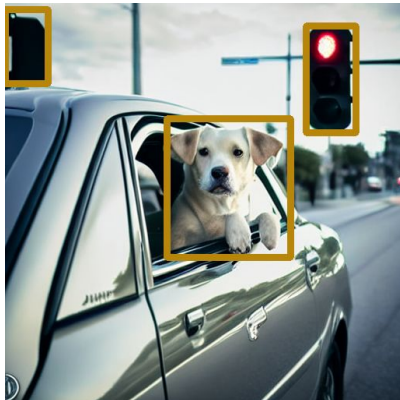
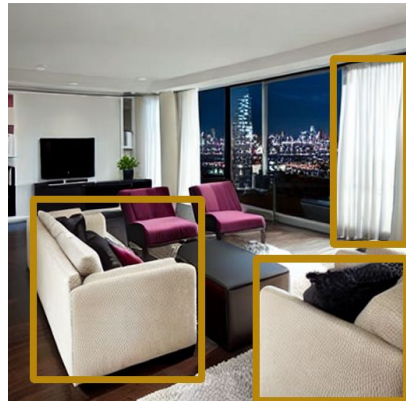
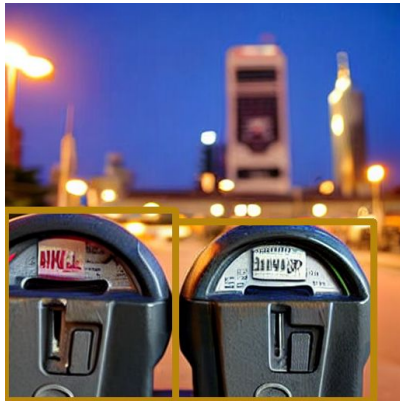


Figure G. Zooming in ReCo_{LAION}-generated images shown in Figure B.

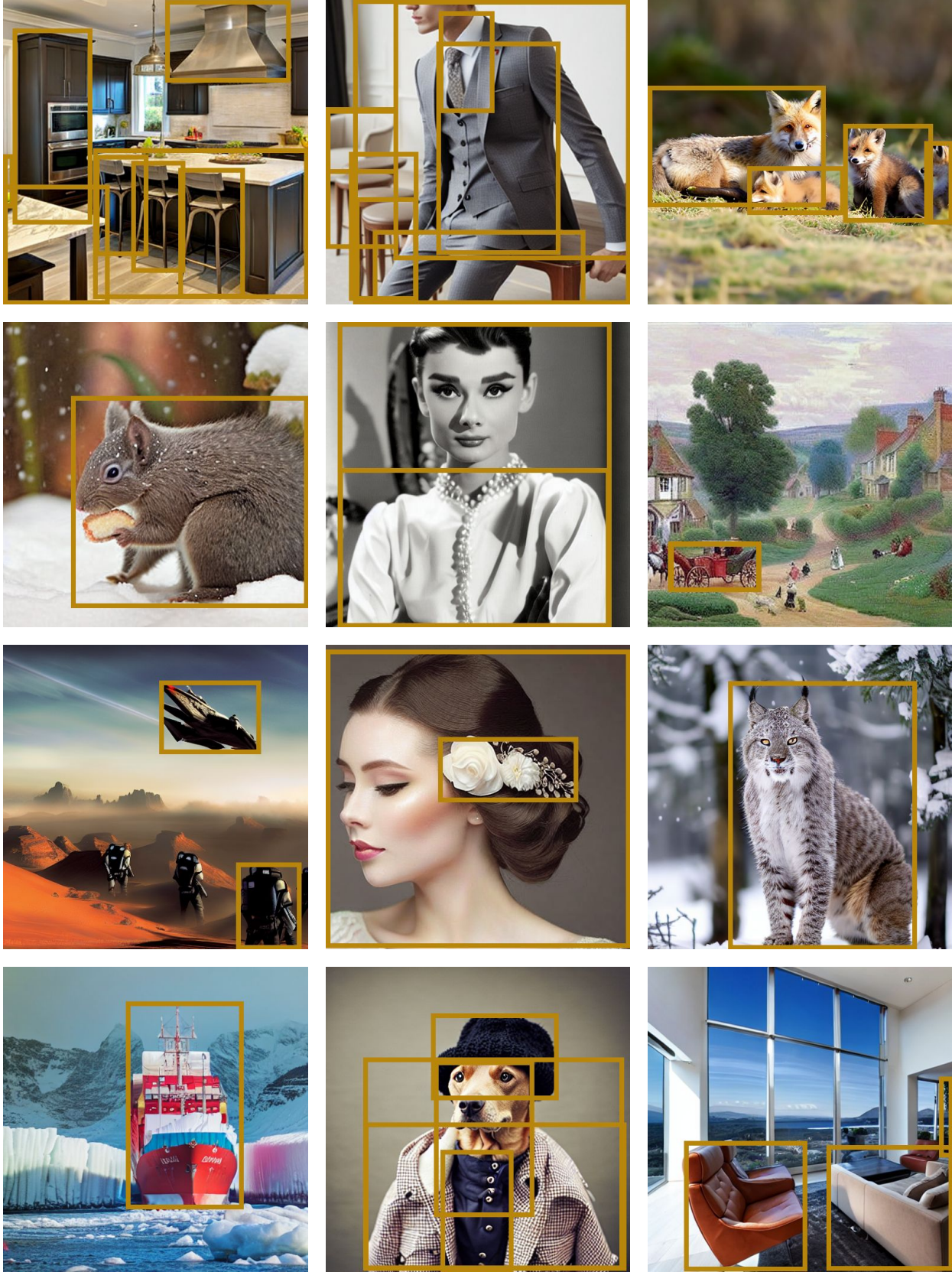


Figure H. Zooming in ReCo_{LAION}-generated images shown in Figure C.

- [2] Agrim Gupta, Piotr Dollar, and Ross Girshick. Lvis: A dataset for large vocabulary instance segmentation. In *CVPR*, 2019. [2](#), [3](#), [4](#)
- [3] Yash Kant, Dhruv Batra, Peter Anderson, Alex Schwing, Devi Parikh, Jiasen Lu, and Harsh Agrawal. Spatially aware multi-modal transformers for textvqa. In *ECCV*, 2020. [5](#)
- [4] Robin Rombach, Andreas Blattmann, Dominik Lorenz, Patrick Esser, and Björn Ommer. High-resolution image synthesis with latent diffusion models. In *Proceedings of the IEEE/CVF Conference on Computer Vision and Pattern Recognition*, pages 10684–10695, 2022. [1](#), [5](#)
- [5] Christoph Schuhmann, Romain Beaumont, Cade W Gordon, Ross Wightman, Theo Coombes, Aarush Katta, Clayton Mullis, Patrick Schramowski, Srivatsa R Kundurthy, Katherine Crowson, et al. Laion-5b: An open large-scale dataset for training next generation image-text models. In *Thirty-sixth Conference on Neural Information Processing Systems Datasets and Benchmarks Track*, 2022. [1](#), [2](#), [3](#)
- [6] Jianfeng Wang, Zhengyuan Yang, Xiaowei Hu, Linjie Li, Kevin Lin, Zhe Gan, Zicheng Liu, Ce Liu, and Lijuan Wang. Git: A generative image-to-text transformer for vision and language. *arXiv preprint arXiv:2205.14100*, 2022. [2](#)
- [7] Peng Wang, An Yang, Rui Men, Junyang Lin, Shuai Bai, Zhikang Li, Jianxin Ma, Chang Zhou, Jingren Zhou, and Hongxia Yang. Ofa: Unifying architectures, tasks, and modalities through a simple sequence-to-sequence learning framework. In *International Conference on Machine Learning*, pages 23318–23340. PMLR, 2022. [5](#)
- [8] Ting Yao, Yingwei Pan, Yehao Li, and Tao Mei. Exploring visual relationship for image captioning. In *ECCV*, 2018. [5](#)
- [9] Xingyi Zhou, Rohit Girdhar, Armand Joulin, Philipp Krähenbühl, and Ishan Misra. Detecting twenty-thousand classes using image-level supervision. In *European Conference on Computer Vision*, pages 350–368. Springer, 2022. [1](#)